

UDK 535.215:548.55:661.852

Photoacoustic Properties of Single Crystal PbTe(Ni)

D. Luković^{1,*}, P.M. Nikolić¹, S. Vujatović¹, S. Savić¹, D. Urošević²

¹Institute of Technical Sciences of SASA, Knez Mihailova 35/IV, 11000 Belgrade, Serbia

²Mathematical Institute of SASA, Knez Mihailova 35/I, 11000 Belgrade, Serbia

Abstract:

Single crystals of PbTe(Ni) were investigated by the photoacoustic method. They were produced using the Bridgeman method. These crystals have a sodium chloride cubic lattice and could be cleaved parallel to the plane orientation (200). They were of the n-type. Phase and amplitude photoacoustic spectra were measured using a transmission detection configuration set-up. Photoacoustic (PA) spectra (single and normalized) were numerically analyzed using the Rosencwaig-Gersho model. Thermal diffusivity and some electron-transport parameters were determined. These results were compared with existing results for pure single crystal PbTe. Thermal diffusivity of PbTe(Ni) is a bit higher than the thermal diffusivity of pure PbTe. This is the consequence of a decreasing concentration of the majority free carriers in the doped alloy.

Keywords: *Photoacoustic method, Thermal diffusivity, Minority free carrier mobility.*

Introduction

Lead telluride, PbTe, is a narrow-gap semiconductor used in optoelectronics for the production of lasers and LED's, working in the FIR range. PbTe doped with various impurities has been frequently studied [1, 2, 3]. Also, these materials are useful for producing IR detectors resistant to nuclear radiation. The energy gap of single crystal PbTe varies with temperature and it is 0.32 eV at room temperature. It has a sodium-chloride cubic crystal lattice. Undoped single crystals of PbTe have a high charge carrier concentration because of the deviation of composition from stoichiometry. Doping of PbTe with some elements results in a decrease of the carrier concentration.

Experimental

Single crystal ingots of PbTe doped with the starting composition of 3 at% Ni were synthesized using the Bridgman method. The Ni contents in our samples of PbTe(Ni) were determined using scanning electron microscopy and emission spectroscopic analysis. The nickel content in the first sample was 0.29 % (SEM). The exact value of Ni in the second sample was not determined, but estimated, according to emission spectroscopic analysis, as approximately three times larger than in the first sample. In the following text these samples will be marked as A and C, respectively.

*) Corresponding author: danijela@bib.sanu.ac.yu

X-ray diffraction analysis confirmed that the samples were single crystals and it was indicated that they were cleaved parallel to the (200) plane.

Hall measurements at room temperature showed that our samples were of the *n*-type. The values of electron concentration and mobility of electrons obtained by this method were: $n(A)=9.1\times 10^{15} \text{ cm}^{-3}$, $\mu(A)=2.8\times 10^3 \text{ cm}^2/\text{Vs}$, $n(C)=2.4\times 10^{16} \text{ cm}^{-3}$, $\mu(C)=1.1\times 10^3 \text{ cm}^2/\text{Vs}$. Therefore, the sample *A* (with a smaller amount of Ni) has a lower concentration and larger mobility of electrons than sample *C* (with a larger amount of Ni).

Both samples were cleaved from an ingot and their surfaces were polished with SiC sand paper.

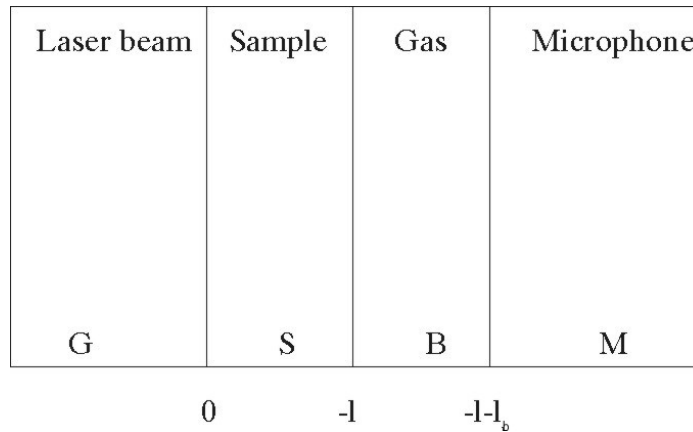


Fig. 1 The gas-sample-backing-microphone (transmission detection) configuration of a PA cell

Photoacoustic (PA) phase and amplitude spectra of single crystal samples were measured using a photoacoustic cell with a transmission detection configuration (Fig. 1). A semiconducting red laser (10 mW) was used as an optical source and the laser beam was modulated with a mechanical chopper. The PA signal was measured in the frequency range of modulation from 7 Hz to 400 Hz for two different sample thicknesses.

Results and Discussion

The phase and amplitude PA spectra of PbTe doped with Ni versus the modulating frequency are given in Fig. 2 for two different thicknesses of sample *A* (470 μm and 390 μm). It can be seen that the phase diagrams exhibit a minimum at the characteristic frequency of modulation and amplitude diagrams exhibit a change of curve slope at the same frequency. The sample behaves as thermally thin at frequencies lower than this characteristic frequency

i.e. the sample thermal diffusion length $\mu = \left(\frac{D_T}{\pi f} \right)^{1/2}$ is larger than the sample thickness

($l \ll \mu$). At higher frequencies the sample behaves as thermally thick ($l \gg \mu$).

Numerical analysis of experimental PA results was based on the Rosencwaig-Gersho [4] thermal piston model modified by taking into account the carrier transport properties [5]. This model includes three mechanisms which contribute to the PA signal: thermodiffusion (TD), thermoelastic (TE) and electronic deformation (ED) mechanism. The first one is a result of thermal wave propagation through a sample and surrounding gas (which is in contact with the sample). These thermal waves also produce elastic vibrations of the sample surface, which cause expansion and contraction of the surrounding gas (acoustic wave). This is the

thermoelastic mechanism of PA signal generation. The photoexcited free carriers generate mechanical straining in the sample and periodic elastic deformation that, like the others, also generates an acoustic wave.

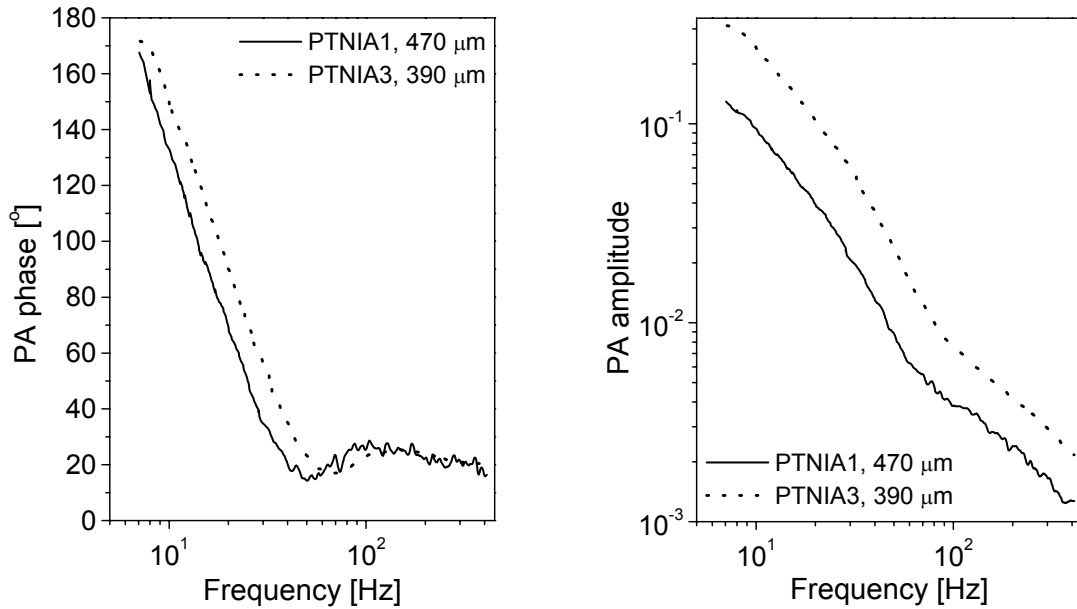


Fig. 1 Phase and amplitude diagrams vs modulation frequency for two different thicknesses of single sample PbTe(Ni), *A*

The thermodiffusion component of the PA signal is a consequence of a heat conduction process in sample. It depends on the periodic temperature variation of the rear side of sample which is in contact with electret microphone. This component of the PA signal can be expressed as:

$$S^{TD}(-l, \omega) = \frac{\gamma P_0}{T_0 k_b l_b} \Phi_s(-l_s, \omega) \quad (1)$$

where l is the sample thickness, ω is the frequency modulation of the light laser beam; γ is the adiabatic constant; P_0 and T_0 are the ambient pressure and temperature, respectively; $k_b = (1+j)/\mu_b$, where μ_b is the thermal diffusion length of the backing gas; l_b is the distance between the sample and microphone membrane; $\Phi_s(-l_s, \omega)$ is the temperature variation of the sample surface that is in contact with the microphone.

The PA signal can be expressed by the following relation:

$$S(-l, \omega) = c_{td} [\Phi^T(-l) + \Phi^{BR}(-l) + \Phi^{SR}(-l)] \quad (2)$$

where c_{td} is the thermodiffusion constant, l is the sample thickness, Φ^T , Φ^{BR} and Φ^{SR} are the fast thermalization component, slow bulk recombination component and surface recombination component of the periodic temperature, respectively. The thermalization component Φ^T is dominant at low frequencies, but at the intermediate and high frequencies excess carrier diffusion and recombination processes dominate. Therefore, the PA signal is

practically characterized at low frequencies only by the thermal processes and by carrier transport processes at intermediate and high frequencies.

Numerical analysis of experimental PA spectra by a fitting procedure gave as a result values of some thermal and electronic transport parameters: thermal diffusivity D_T , minority carrier diffusion coefficient D , optical absorption coefficient α , excess carrier lifetime τ , front s_g and rear s_b surface recombination velocity. The fitting program enables us to choose the values of the parameters in the previously given theoretical model for PA measurements. One can select the magnitude of change of each parameter and also fitting criteria. The fitting error can be calculated using one of four criteria.

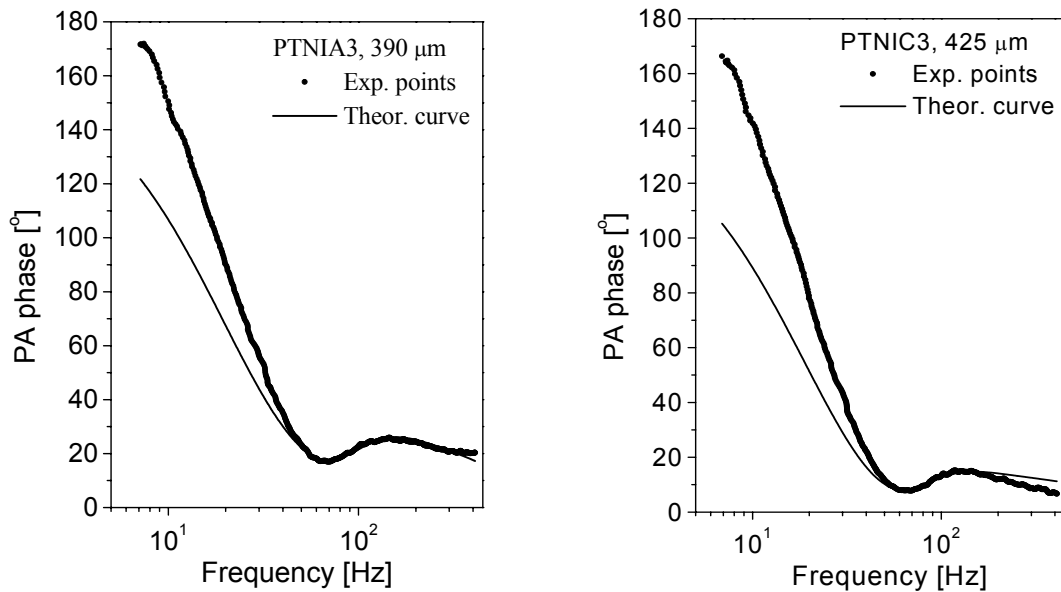


Fig. 3 Phase (a) and amplitude (b) PA experimental (dots) and theoretical (line) diagrams as a function of modulation frequency for a PbTe(Ni) single crystal sample, A

Experimental and theoretically fitted phase PA diagrams were represented in Fig. 3 for samples A and C , respectively. The values of some thermal and transport parameters obtained from the fitting procedure for both PA spectra are given in Tab. I.

Phase and amplitude PA diagrams should be corrected in the frequency range below 100 Hz because the electret microphone sensitivity is lower in this frequency range. Influences of device and environment can be eliminated by a normalizing procedure. Experimental PA spectra of the same sample but for two different thicknesses were used for calculation of the PA signal ratio:

$$\frac{S_1(\omega)}{S_2(\omega)} = \frac{\Phi(-l_1)}{\Phi(-l_2)} \exp j[\varphi(-l_1) - \varphi(-l_2)] = A_n \exp j\Delta\varphi_n \quad (3)$$

where $S_1(\omega)$ and $S_2(\omega)$ are the PA signals for the different thicknesses of the sample, A_n is the amplitude ratio and $\Delta\varphi_n$ is the phase difference of these two PA signals. These normalized experimental PA phase and amplitude diagrams can then be fitted with the theoretically calculated PA signals. The values of parameters obtained from the fitting procedure of

normalized PA diagrams are also given in Tab.I Fig. 4 shows the fitting theoretical and normalized experimental PA phase and amplitude spectra for sample C.

Tab. I PA parameters obtained by numerical analysis for samples PbTe(Ni) –A and C

	Sample A			Sample C		
	PTNIA1	PTNIA3	PTNIA1/ PTNIA3	PTNIC1	PTNIC3	PTNIC1/ PTNIC3
d [μm]	470	390	470/390	685	425	685/425
D_T [m^2/s]	1.86×10^{-6}	1.86×10^{-6}	1.86×10^{-6}	1.64×10^{-6}	1.63×10^{-6}	1.64×10^{-6}
D [m^2/s]	2.25×10^{-3}	2.38×10^{-3}	2.38×10^{-3}	2.18×10^{-3}	2.18×10^{-3}	2.18×10^{-3}
μ_p [cm^2/Vs]	8.7×10^2	9.2×10^2	9.2×10^2	8.4×10^2	8.4×10^2	8.4×10^2
τ [s]	3.24×10^{-4}	2.35×10^{-4}	3.15×10^{-4}	3.81×10^{-5}	1.74×10^{-4}	1.36×10^{-4}
α [m^{-1}]	2.6×10^4	9.6×10^4	2.6×10^4	9.2×10^4	1.6×10^4	1.8×10^4
s_b [m/s]	0.9	3.1	1.3	24.2	10.3	105
s_g [m/s]	0.4	0.64	0.42	25.3	48	45

The values of thermal diffusivity D_T were independent of samples' thicknesses. They were of the same order of magnitude ($\sim 10^{-6} \text{ m}^2/\text{s}$) but $D_T(A) > D_T(C)$. Contribution of the free carriers to thermal diffusivity is larger in sample A because the electron concentration is lower than in sample C.

These results were also compared with existing results for pure single crystal PbTe [6]. One can conclude that thermal diffusivity of PbTe(Ni) is a bit higher than the thermal diffusivity of pure PbTe, $D_T(\text{PbTe}) = 1.55 \times 10^{-6} \text{ m}^2/\text{s}$. This is the consequence of a decreasing concentration of the majority free carriers in the doped alloy.

The values of absorption coefficient α were relatively high. These results are acceptable because the energy of the laser beam ($E = 1.96 \text{ eV}$) was multiply greater than the energy gap of the material ($E_g = 0.32 \text{ eV}$). The energy gap of PbTe(Ni) was practically the same as the energy gap of pure PbTe.

The diffusion coefficient of minority free carriers is smaller for sample C ($D = \frac{\mu kT}{e}$) and that means that the mobility of free carriers is smaller. That is in agreement with the measurements of electrical properties. Another confirmation of these results is that the excess carrier lifetime is also smaller for sample C than A.

The values of diffusion coefficient D are the same order of magnitude for both samples ($\sim 10^{-3} \text{ m}^2/\text{s}$) and they are as expected higher for sample A than for sample C.

Minority free carrier (hole) mobility μ_p is larger for sample A which has a lower concentration of carriers. These values were also larger than hole mobility in pure PbTe that is $750 \text{ cm}^2/\text{Vs}$ [7].

Front s_g and rear s_b surface recombination velocities of each sample did not differ much because both sides were polished, but unequally well.

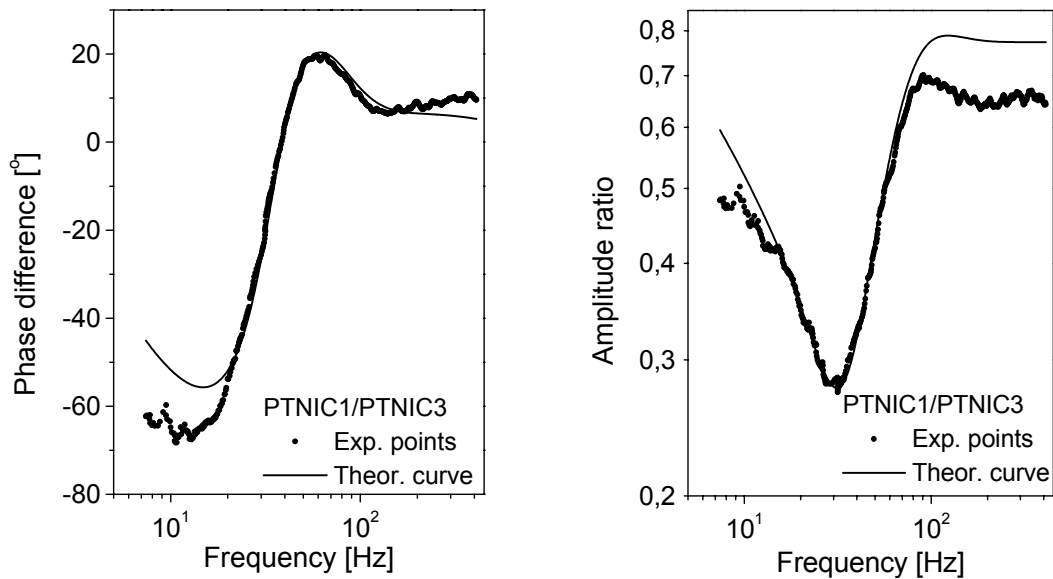


Fig. 4 Phase (a) and amplitude (b) PA experimental (dots) and theoretical (line) diagrams as a function of modulation frequency for a PbTe(Ni) single crystal sample, *C*

Conclusion

This work was done as a result of an investigation of some thermal and electron transport properties (parameters) of PbTe(Ni) samples with nickel contents below 1% by the photoacoustic method. The thermal diffusivity D_T and minority free carriers' (holes') mobility μ_p were obtained by numerical analysis of experimental PA spectra. It was shown that they were both larger for the sample with the lower carrier concentration though values of thermal diffusivity for both samples were of the same order of magnitude ($D_T \sim 10^{-6} \text{ m}^2/\text{s}$, $\mu_p \sim 10^2 \text{ cm}^2/\text{Vs}$). They were also larger, but the same order of magnitude, for our doped samples than for pure PbTe because of lowering of carrier concentration by doping.

References

1. V.I. Kaidanov, J. I. Ravich, Usp. Fiz. Nauk, 145 (1985) 51.
2. B.A. Akimov, A.V. Dmitriev, D.R. Khokhlov, L.I. Ryabova, Phys. Status Solidi A, 137 (1993) 9.
3. A. Lambrecht, H. Bottner, M. Agne, R. Kurbel, A. Fach, B. Halford, U. Schiessl, M. Tacke, Semicond. Sci. Technol., 8 (1993) S334.
4. A. Rosencwaig, A. Gersho, J. Appl. Phys., 47 (1976) 64.
5. D.M. Todorović, P.M. Nikolić, A.I. Bojičić, K.T. Radulović, Phys. Rev. B, 55 (1997) 15631.
6. P.M. Nikolić, D. Vasiljević, M. Miletić, *Glas CCCLXXX Srpske akademije nauka i umetnosti Odeljenje tehničkih nauka knj.32-1996* (in Serbian).
7. P.M. Nikolić, D. Raković, *Elektrotehnički materijali*, Naučna knjiga, Beograd 1987 (in Serbian).

Садржај: Монокристал $PbTe$ (Ni) је испитиван фотоакустичном методом. Монокристали овог материјала су начињени Брицмановом методом. Ови кристали имају натријум-хлоридну кубну кристалну решетку и могу се сећи паралелно равни оријентације (200). Узорци $PbTe(Ni)$ су n -типа. Фотоакустични спектри су нумерички анализирани помоћу Розенцвајг-Гершо модела. Одређена је топлотна дифузивност као и неки електронски транспортни параметри ових узорака. Добијени резултати су упоређени са постојећим подацима за чист монокристал $PbTe$. Топлотна дифузивност $PbTe$ допираног са Ni је нешто већа него топлотна дифузивност чистог $PbTe$, што је последица смањења концентрације већинских слободних носилаца у допираном $PbTe$.

Кључне речи: Фотоакустична метода, топлотна дифузивност, покретљивост мањинских слободних носилаца.
